Desalination and Water Treatment
www.deswater.com

doi: 10.1080/19443994.2015.1062432

57 (2016) 14169–14177
June

Taylor & Francis
Taylor & Francis Group

A solid waste, crashed autoclaved aerated concrete, as a crystalline nucleus for the removal of low concentration of phosphate

Weijie Li, Lixuan Zeng*, Yuan Kang, Qiuyun Zhang, Jiwen Luo, Xingmei Guo

Key Laboratory of Theoretical Chemistry of Environment, Ministry of Education, School of Chemistry and Environment, South China Normal University, 378 Waihuan West Road, Guangzhou 510006, China, Tel. +86 20 13640221972; emails: liweijie@m.scnu.edu.cn (W. Li), zenglx@scnu.edu.cn (L. Zeng), kangyuan407@gmail.com (Y. Kang), hnsdhks@163.com (Q. Zhang), holdit@126.com (J. Luo), 517123069@qq.com (X. Guo)

Received 12 February 2015; Accepted 8 June 2015

ABSTRACT

In this study, crashed autoclaved aerated concrete (CAAC) was recycled as a solid waste for the removal of low concentration of phosphate (1 mg/L). The effects of dissolved calcium (Ca^{2+}) and pH on phosphate removal were investigated. The materials including calcium chloride ($CaCl_2$) and calcium carbonate ($CaCO_3$) were selected to investigate the removal mechanism of low concentration of phosphate by CAAC. X-ray fluorescence, X-ray diffraction patterns, FT-IR, SEM, and EDS analyses were used to characterize the surface shape, contained elements, and internal structure of CAAC. Results showed that the removal rate of phosphate was increased according to the increase in pH. The CAAC showed poor effect on phosphate removal at acidic condition, but had great removal efficiency in the pH range of 10–12 due to the formation of hydroxyapatite (HAP, $Ca_5(OH)(PO4)_3$) corresponding to characterization. Dissolved calcium and insoluble calcium compounds in CAAC can combine with the phosphate and hydroxyl groups to form HAP in alkaline condition and subsequently remove the phosphate. SEM images exhibited the surface of CAAC including some pieces of irregular crystal. After phosphate removal, its surface was covered with a layer of agglomerations confirmed to be HAP according to characterization. To avoid adjusting the pH of solution to strong alkalinity, CAAC was modified by sodium hydroxide solution (NaOH) to increase its activity. Modified products showed a high efficiency for phosphate removal (98.67%). Collectively, the present results demonstrated that the employment of crystallization using CAAC could be a promising technology for the advanced treatment of phosphate from low concentration in municipal secondary effluent.

Keywords: Crashed autoclaved aerated concrete; Low concentration of phosphate; Removal mechanism; Hydroxyapatite; Modified

1. Introduction

The environmental issue of eutrophication has become the world matter of concern. Phosphate and nitrate are the major nutrients causing eutrophication, where the former is more important. Moreover, phosphate concentration is a significant factor to control the growth of algae. Now, the presence of trace amounts of phosphate (even less than 1 mg/L) in treated wastewater from municipalities and industries is

---

*Corresponding author.

often responsible for eutrophication, which gives rise to short- or long-term environmental and esthetic problems in lakes, areas, and other confined water bodies. Several studies have shown that the discharge of 0.2 mg/L phosphate into the surface waters would stimulate the growth of aquatic micro- and macro-organisms in nuisance quantities and subsequently result in eutrophication [1,2]. In order to meet the effluent quality standards, advanced treatment for secondary effluent is required. In wastewater treatment technology, various techniques have been used in phosphate removal. Among these, chemical and biological methods have been successfully applied [3–7]. However, the chemical way results in a large amount of reagent consumption, operation cost, and sludge production and the biological treatment occupies a large area of lands with high investment. Accordingly, exploring a sustainable and affordable technology for the advanced treatment of low concentration of phosphate in secondary effluent is necessary.

Crystallization may serve as a promising solution for phosphate removal. One of the main advantages is that the crystal only generate on the surface of crystalline nucleus, which will not produce a large quantity of sludge. When crystalline reaction is used for phosphate removal, the selection of materials as crystalline nucleus is an important factor. Among these, most of mineral materials containing calcium (such as convert slag and Polonite) are widely employed to remove phosphate [8–15]. The mechanism of crystallization is that calcium, phosphate, and hydroxyl ions can react with each other to form alkaline hydroxyapatite (HAP, $Ca_5(OH)(PO_4)_3$). The reaction equation is as follow:

$$5Ca^{2+} + 3HPO_4^{2-} + 4OH^- \rightarrow Ca_5(OH)(PO_4)_3\downarrow + 3H_2O \quad (1)$$

$$5Ca^{2+} + 3PO_4^{3-} + OH^- \rightarrow Ca_5(OH)(PO_4)_3\downarrow \quad (2)$$

As shown in above equations, the PO_4-P in the aqueous solution phase can be continuously removed from solution by bonding with the calcium (Ca^{2+}) and hydroxyl ion (OH^-). It is illustrated that Ca^{2+} and OH^- are the important parameters for phosphate removal. Furthermore, HAP once formed would not be easily released in a short time due to its low solubility, which can attain the goal of phosphate removal and recovery.

Autoclaved aerated concrete (AAC, Fig. 1), a widely used building material, is made of simple or even waste ingredients (sand and fly ash) and mineral binders (lime and cement). In view of its characteristics of higher calcareous materials, its porous, and alkaline conditions, AAC with a certain range of particle diameter size has been reported to purify and recover the phosphate in wastewater [16–20]. To date, however, little research has been conducted on the utilization of AAC for the advanced treatment of low concentration of phosphate.

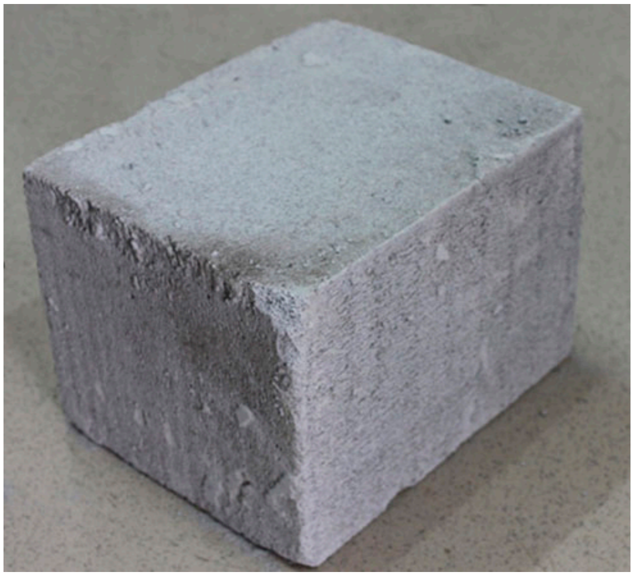

Fig. 1. Autoclaved aerated concrete (AAC).

In the present study, crushed autoclaved aerated concrete (CAAC, Fig. 2), waste residues from the manufacturing process of AAC, was used as original experimental materials to remove low-concentrated phosphate (1 mg/L). The specific objectives of this study were to evaluate the mechanism of phosphate

Fig. 2. Crashed autoclaved aerated concrete (CAAC).

removal, to investigate the major influencing factors (Ca^{2+} and pH), to qualitatively elucidate the phenomenon of calcium phosphate precipitation through a series of characterization. And to further improve the removal rate of phosphate by modification.

2. Materials and methods

2.1. Materials and reagents

The standard phosphate solution with concentration of 1 mg/L-P which is close to the second effluent was prepared from anhydrous KH_2PO_4.

CAAC used in this study (Fig. 2) was obtained from a building materials factory in Guangzhou, China. The chemical composition of CAAC obtained by X-ray Fluorescence (XRF) is shown in Table 1. The most abundant components in CAAC are found to be the oxides of SiO_2 (48.11%) and CaO (28.59%), which are the constituents of CAAC framework. The CAAC was used as a powder obtained by grinding and sieving through a 100-mesh sieve.

CAAC modified by NaOH was prepared according to the following reaction conditions: reaction time 2 h, liquid/solid ratio 5 mL/g (100 mL/20 g), NaOH concentration 2 M, and temperature 25℃. After 2 h reaction, modified materials were recovered by centrifugation and washed three times with distilled water and twice with ethanol. Finally, the products were dried in an oven at 45℃, ground to pass through a 100-mesh sieve, and stored in airtight containers for later experiments.

All chemicals and reagents used were of analytical reagent grade. All glassware and sample bottles were soaked in diluted hydrochloric acid (HCl) solution for 12 h, washed and then rinsed four times with deionized water. Deionized water was used for preparing all the solutions.

2.2. Experiment methods

Experiment was carried out by shaking 50 mL of 1 mg/l KH_2PO_4 (as P) solution at 200 rpm with 0.5 g of materials in the bottles capped with glass screws for 2 h (reaction time of 2 h was found to be enough for phosphate to achieve equilibrium in pre-experiments) at 25℃. The pH was adjusted to a given value by adding HCl or NaOH. After being shaken for 2 h, the suspensions were subsequently centrifuged and the supernatants were determined for phosphate by the molybdenum-blue ascorbic acid method. The Ca^{2+} concentrations were confirmed by calcium-EDTA titrimetric method. The pH in aqueous solution was measured using a pH meter with glass electrode. The residue after centrifuged was dried in an oven at 45℃ and stored in airtight containers for later experiments. All experiments were conducted in duplicate and the average values were used for data analysis.

2.3. Analytical methods

The chemical composition of CAAC was determined by energy dispersive XRF (PW2404, PHILIPS Company). The X-ray Diffraction patterns (XRD) were recorded using BRUKER D8 ADVANCE (German). FT-IR spectra were done by Nicolet 6700 (America). The physicochemical properties of the CAAC before and after reaction were determined using scanning electron microscopy (SEM) (Zeiss Ultra 55, German) and energy dispersive X-ray analysis (EDX) (Oxford X-Max 50) techniques to microscopically investigate the mechanism in phosphate removal.

3. Results and discussion

3.1. The influencing factors for the removal of low concentration of phosphate using CAAC

3.1.1. Blank experimental effect

From Eqs. (1) and (2), Ca^{2+} and OH^- are the most important factors for the formation of HAP in phosphate removal. Moreover, CAAC as an alkaline material is composed mainly of stable calcium–silicate–hydrate phases (CSH-phases), which are hard to be dissolved. Therefore, CAAC in this study was added into deionized water to investigate the variation of Ca^{2+} concentrations and pH in solution.

As shown in Fig. 3, at the condition of solid/liquid ratio of 10 g/L (0.5 g/50 mL), the Ca^{2+} concentration and pH in aqueous solution increases with the extension of time and reaches equilibrium at about 30 and 20 min, respectively. The result shows that though

Table 1
Chemical composition of CAAC

Compound (%)	SiO_2	Al_2O_3	Fe_2O_3	CaO	MgO	K_2O	Na_2O	SO_3
AAC	48.11	8.25	5.39	28.59	0.74	0.72	0.19	0.67

CAAC is composed mainly of stable CSH-phases, it can release a faction of dissolved calcium and alkalinity when soaked in solution, which facilitates the formation of calcium phosphate precipitations.

3.1.2. Ca^{2+} effect

From Eq. (1), it is shown that Ca^{2+} is one of important factors for the formation of HAP in phosphate removal. Hence, the effect of additive Ca^{2+} concentration on phosphate removal was investigated in Fig. 4.

The pH of KH_2PO_4 solution was adjusted to neutral before adding $CaCl_2$. As shown in Fig. 4, the removal rate of phosphate increases slowly with the increase in Ca^{2+} concentration. The result indicates that only increasing Ca^{2+} concentration is unable to improve the removal rate effectively in the present pH value.

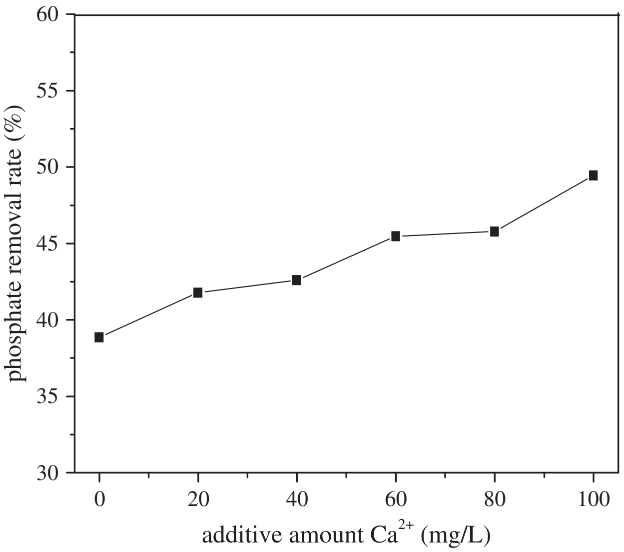

Fig. 4. Effect of Ca^{2+} concentration on phosphate removal.

3.1.3. pH effect

The pH is another important factor for the formation of HAP in phosphate removal. As shown in Eqs. (1) and (2), the PO_4-P can be continuously removed from the solution by combining with the Ca^{2+} and OH^-. According to the XRD analysis, CAAC is made up of insoluble compounds containing calcium and silicon which are possible to transform into another more difficult dissolved substance (HAP) under certain conditions. Therefore, these insoluble calcium compounds and dissolved calcium ion were independently investigated to determine the mechanism of CAAC in phosphate removal. In this study, $CaCO_3$ and $CaCl_2$ were selected. The effect of pH on phosphate removal for above materials was shown in Fig. 5. The initial pH of solution was 2.87 without adjusting by HCl or NaOH.

As shown in Fig. 5, the removal rates of phosphate for three materials generally increase with the increase in pH. In addition, the phosphate removals for three materials are greatly effective when the pH is higher than 10 and reach maximum value of 12. The results show that $CaCl_2$ and $CaCO_3$ have a high efficiency for phosphate removal in the pH range of 10–12, which is ascribed to the formation of HAP. Similarly, CAAC

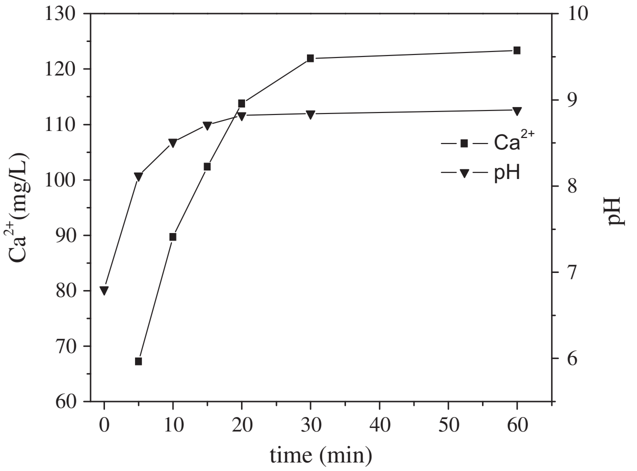

Fig. 3. Variation of Ca^{2+} concentrations and pH in blank experiment.

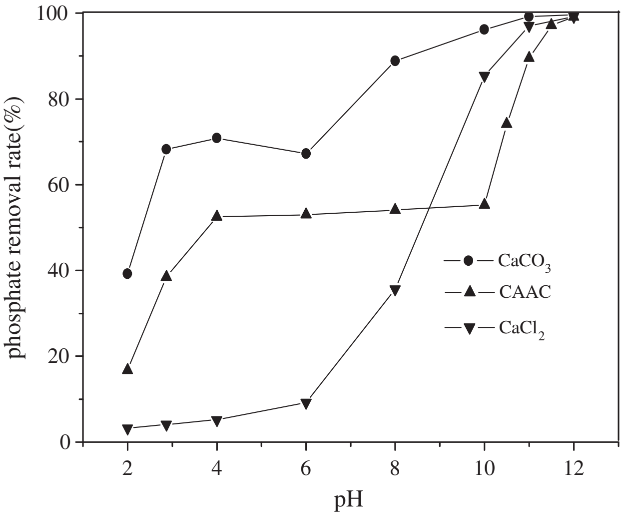

Fig. 5. Effect of pH on phosphate removal for three materials.

also has a same effect on phosphate removal. The following series of analyses are to further illustrate the removal mechanism of phosphate for CAAC.

When the pH increases from 2 to 4 and 10 to 12, the slope is much larger than that in the pH range of 4–10, where the removal rate is kept steady. At the pH of 2, though insoluble calcium compounds in CAAC such as $CaCO_3$ will be dissolved to release Ca^{2+}, the phosphate groups in aqueous solution exist as H_3PO_4 which hardly bonds with Ca^{2+}. Besides, the surface charge of CAAC is also influenced at strong acidic condition. When the pH increases from 2 to 4, the phosphate removal increases, which can be considered that physical adsorption of CAAC plays a dominating role for phosphate removal in this pH range. In the pH range of 4–10, the removal rate is kept steady, which may be explained by that physical adsorption of CAAC reaches equilibrium and this pH range is unable to meet the requirements for the formation of HAP. In this range, $H_2PO_4^-$ and HPO_4^{2-} are the primary phosphate groups in solution, which can combine Ca^{2+} to form calcium phosphate compounds (such as $CaHPO_4$), but hard to form crystalline precipitation due to their low solubility. The removal rate of phosphate greatly increases in the pH range of 10–12, where the high pH can cause PO_4-P to precipitate quantitatively as calcium phosphates [8].

The result shows that if the pH reaches certain value, dissolved calcium ion and insoluble calcium compounds in CAAC will transform into HAP by combining the phosphate and hydroxyl groups to achieve the aim of phosphate removal. In the range of 10–12, HPO_4^{2-} is the main phosphate groups with a faction of PO_4^{3-} in solution and the major reactions are shown in Eqs. (1) and (2).

Among the equations, the Eq. (1) is the most important. However, this pH range for the formation of HAP in the removal of low concentration of phosphate differed from the previous research [14], where the optimal pH range was 8.0–9.5. This distinction is possibly attributed to the difference of material and reaction conditions. In general, the above results indicate that there is a strong relationship between pH and phosphate removal. The removal rate is relatively efficient at alkaline conditions which are benefit to the formation of HAP. Collectively, the removal mechanism of low concentration of phosphate for CAAC includes physical adsorption and crystalline precipitation, where the latter is more significant. When the dosage was 10 g/L, initial phosphate concentration was 1 mg/L, and the pH was in the range of 10–12, CAAC showed great effect on phosphate removal.

3.2. Characterization

SEM, XRD, FT-IR, and EDS analyses were conducted to investigate the physicochemical properties of CAAC before and after phosphate removal. These series of characterization are to further determine the removal mechanism of low concentration of phosphate by CAAC.

3.2.1. SEM analysis

The surfaces of the CAAC before and after phosphate removal are depicted in Figs. 6 and 7, respectively. Fig. 6 shows the magnified SEM micrograph of CAAC before phosphate removal contains a number of irregular sheet particles mostly composed of CSH-phases according to XRD analysis. These sheet particles might be hollow particles filled with smaller pieces which are linked with the inner part of the particles. Fig. 7 shows the surface of CAAC after phosphate removal is covered with a layer of agglomerations. This phenomenon could be explained by that phosphate removal using CAAC may firstly go through a process of flocculent precipitation then the calcium phosphate crystalline precipitation will generate on the surface of CAAC to change its superficial shape [15]. According to the XRD and FT-IR analyses presented below, the appearance of these agglomerations were due to the formation of HAP.

3.2.2. XRD analysis

XRD analysis was conducted to investigate the variation in the crystal structure of the materials

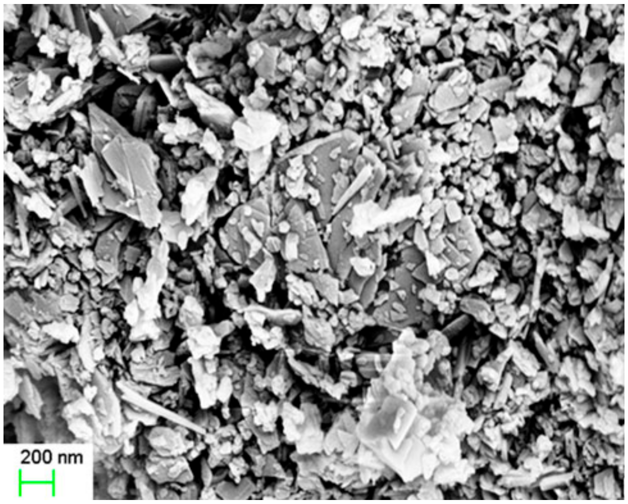

Fig. 6. SEM micrograph of CAAC before phosphate removal.

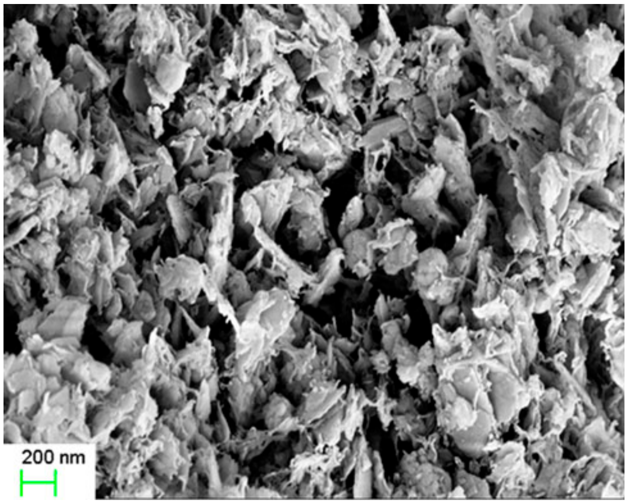

Fig. 7. SEM micrograph of CAAC after phosphate removal.

deposited on the CAAC during the phosphate removal reaction. Fig. 8(a) and (b) shows the XRD patterns for CAAC before and after phosphate removal, respectively. The XRD analysis was performed over a 2*θ* range of 10–70˚.

As shown in Fig. 8(a), the crystalline phases present in CAAC were quartz (SiO_2) and tobermorite ($Ca_5Si_6O_{16}(OH)_2{\cdot}4H_2O$), gypsum ($CaSO_4$), and limestone ($CaCO_3$). The peaks in the 2*θ* range from 20˚ to 35˚ indicated the presence of amorphous component. The amorphous components may contain calcium, iron, and aluminum, which were confirmed in EDS mapping analysis presented below. Comparison of Fig. 8(a) and (b) shows the appearance of two sharp and intense peaks characteristic of HAP ($2\theta = 31.4^\circ$ and 31.9˚) after phosphate removal. Additionally, the reflections of limestone, gypsum, and tobermorite were partly reduced or even absent after reaction, which explained that the ordered structure of them were partially destroyed. Because of that, the Ca^{2+} could be released from CAAC to solution and the insoluble substances (such as $CaCO_3$ and $Ca_5Si_6O_{16}(OH)_2{\cdot}4H_2O$) in CAAC will transform another precipitation (HAP) with lower solubility. XRD results reveal that growth of crystalline HAP on the CAAC causes the amount of order in the particles to increase as phosphate crystallization reaction progresses.

In addition to HAP, the presence of calcium phosphate compounds such as tricalcium phosphate ($Ca_3(PO_4)_2$) and calcium hydrogen phosphate ($CaHPO_4$) was not observed in the XRD pattern due to their lower solubility. According to above analyses, the crystal of HAP will be generated on the surface of CAAC in phosphate removal.

3.2.3. FT-IR analysis

The FT-IR spectra of the CAAC (before and after phosphate removal) were recorded between 400 and 4,000 cm^{-1} in Fig. 9(a) and (b), respectively. The banks at 464, 973 cm^{-1} are assigned to TiO_4, doable ring and T–O bending, respectively (T=Si and Al). The characteristic band related to Fe–O–Fe bond of iron oxide must be appearing at 580 cm^{-1}. Another band

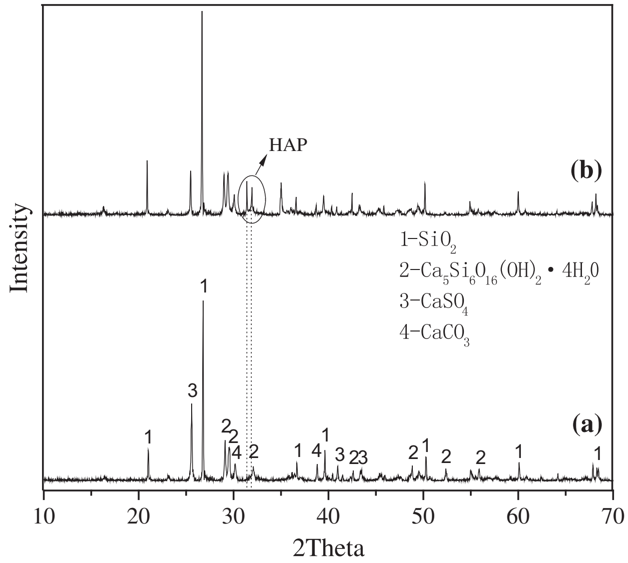

Fig. 8. XRD patterns of CAAC (a) before and (b) after phosphate removal.

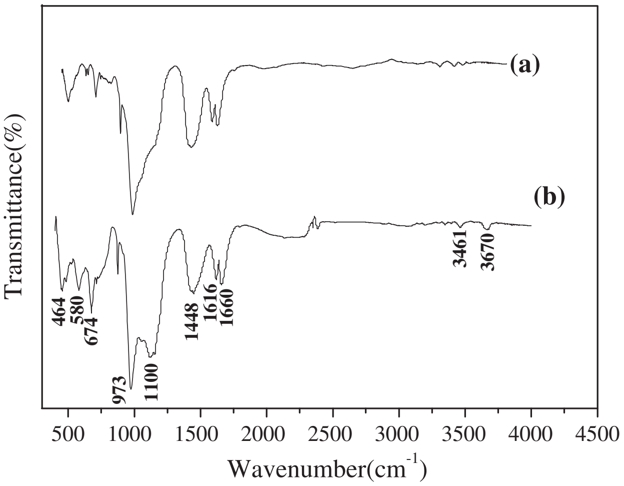

Fig. 9. FT-IR spectra of the CAAC (a) before and (b) after phosphate removal.

observed at 674 cm^{-1} is due to Si–O–Ca bond. The CO_3^- band is detected at around 1,448 cm^{-1}. In addition, the adsorption bands at 1,616 and 1,660 cm^{-1} are related to interstitial bonded water. The FT-IR spectra of CAAC after phosphate removal exhibits new peaks at 1,100 cm^{-1} (corresponding to the $\mathrm{PO4}^{3-}$ vibration) and at 3461, 3670 cm^{-1} (corresponding to the OH^- stretching vibration), which correspond to the characteristic bands of HAP [15]. Similarly, the presence of other calcium phosphate compounds such as $\mathrm{Ca}_3(\mathrm{PO}_4)_2$ and CaHPO_4 is not distinctly observed in the FT-IR spectra of Fig. 9(b) corresponding to the XRD analysis. In a word, the results of FT-IR analyses manifest that the low-concentrated phosphate in wastewater could be removed and immobilized by the formation of HAP.

3.2.4. EDS mapping analysis

EDS mapping analysis was performed to determine the chemical composition of the crystalline materials adhered to the surface of CAAC. The EDS mapping analysis, depicted in Fig. 10, reveals that the surface of flocculent precipitation appears the elements of Ca and P, which support the XRD and FI-IR analyses. In addition, other types of elements such as iron (Fe) and aluminum (Al) are also detected in EDS mapping analysis, which may partly formed as amorphous insoluble precipitation on the surface of CAAC according to the XRD analysis. The presence of silicon (Si) was probably due to the dissolution of silicates in the CAAC. The appearance of carbon (C) and oxygen (O) might be attributed to co-crystallization of calcium carbonate due to the carbonate alkalinity and the reaction equation is as follow:

$$\mathrm{Ca}^{2+} + \mathrm{HCO}^{3-} + \mathrm{OH}^{-} \rightarrow \mathrm{CaCO}_3 \downarrow + \mathrm{H}_2\mathrm{O} \tag{3}$$

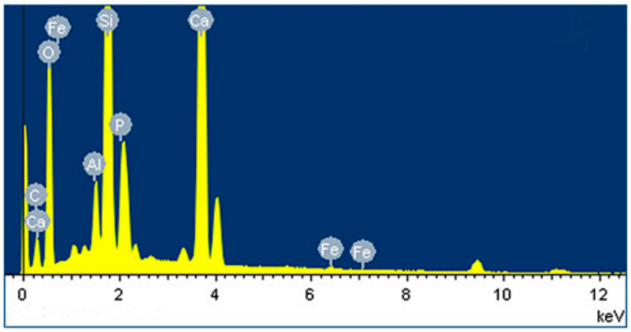

Fig. 10. EDX mapping analysis graph of CAAC after phosphate removal.

3.3. Results of characterization

The results of the XRD, FT-IR, SEM, and EDS analyses indicated that a principal ingredient of the flocculent substances were HAP whose formation are the predominant removal mechanism of low concentration of phosphate using CAAC. Based on the above analyses, CAAC with high content of calcium has the potential to be a cost-effective crystalline nucleus material for phosphate removal.

3.4. CAAC modified by sodium hydroxide solution

The results of the above studies have shown that CAAC has a high efficiency in the removal of low concentration of phosphate at strong alkaline conditions. Actually, it is impossible to adjust the pH of solution to strong alkalinity. Thus, CAAC in this study was modified by NaOH to increase its activity. NaOH can dissolve SiO_2 on the surface of CAAC to facilitate its physical adsorption. In addition, the above analyses show that alkaline condition is beneficial for phosphate removal. SEM micrographs of CAAC after modified by NaOH are shown in Fig. 11.

As shown in Fig. 11, the surface of modified CAAC was coated with some pieces of crystalline materials whose sizes become more uniformly compared to Fig. 6. Effects of CAAC on phosphate removal before and after modification were compared in table 2.

As shown in table 2, the removal rate of phosphate could reach a relative higher level (98.67%) using the modified CAAC. This is due to that the CAAC after modification by NaOH could further increase its

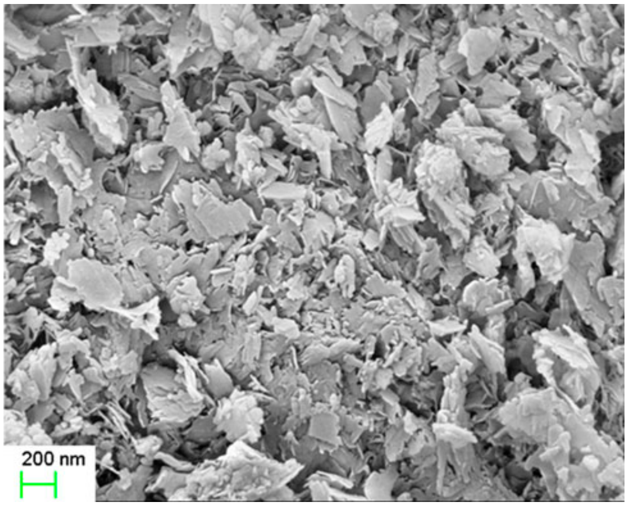

Fig. 11. SEM micrograph of CAAC after modified by NaOH.

Table 2
Effects of CAAC on phosphate removal before and after modification

Materials	Initial pH	Effluent pH	Removal rate of phosphate (%)
CAAC	7.00	8.77	53.51
Modified CAAC	7.00	11.12	98.67

alkalinity, which is shown by the effluent pH. Besides, in this pH range, HPO_4^- as the main phosphate group could bond with Ca^{2+} and OH^- as HAP or other calcium phosphate precipitations. In a word, CAAC modified by NaOH showed a great increase in the removal of phosphate.

4. Conclusion

CAAC as a solid waste was employed to investigate the removal of low concentration of phosphate (1 mg/L). The Ca^{2+} and pH played the critical roles in phosphate removal. When soaked in solution, CAAC can release dissolved calcium and alkalinity. The removal rate of phosphate was increased according to the increase in the pH. The removal mechanism of phosphate using CAAC includes physical adsorption and crystalline precipitation of HAP confirmed by XRD, FT-IR, and EDS mapping analyses, where the latter is more important. Dissolved calcium released by CAAC can combine with PO_4-P and OH^- to form HAP. In addition, insoluble calcium compounds in CAAC can transform into HAP due to its lower solubility. CAAC after modification by NaOH had a high efficiency on phosphate removal (98.67%). Based on above results, CAAC with high content of calcium has the potential to be a new highly efficient and cost-effective material for the advanced treatment of low concentration of phosphate in secondary effluents.

Acknowledgments

This research was supported by the National Natural Science Foundation of China (NO. 21147003) and the Science and Technology Plan Project of Guangdong Province (NO. 2011B030800011)

References

[1] S. Huo, C. Ma, B. Xi, J. Su, F. Zan, D. Ji, Z. He, Establishing eutrophication assessment standards for four lake regions, China, J. Environ. Sci. 25 (2013) 2014–2022.

[2] Z. Wu, Z. Yu, X. Song, Y. Yuan, X. Cao, Y. Liang, Application of an integrated methodology for eutrophication assessment: A case study in the Bohai Sea, Chin J. Oceanol. Limnol. 31 (2013) 1064–1078.

[3] Y. Liu, H. Shi, W. Li, Y. Hou, M. He, Inhibition of chemical dose in biological phosphorus and nitrogen removal in simultaneous chemical precipitation for phosphorus removal, Bioresour. Technol. 102 (2011) 4008–4012.

[4] C. Pratt, S.A. Parsons, A. Soares, B.D. Martin, Biologically and chemically mediated adsorption and precipitation of phosphorus from wastewater, Curr. Opin. Biotechnol. 23 (2012) 890–896.

[5] Y. Yang, Y. Inamori, H. Ojima, H. Machii, Y. Shimizu, Development of an advanced biological treatment system applied to the removal of nitrogen and phosphorus using the sludge ceramics, Water Res. 39 (2005) 4859–4868.

[6] R. Barat, T. Montoya, A. Seco, J. Ferrer, Modelling biological and chemically induced precipitation of calcium phosphate in enhanced biological phosphorus removal systems, Water Res. 45 (2011) 3744–3752.

[7] N.C. Boelee, H. Temmink, M. Janssen, C.J. Buisman, R.H. Wijffels, Nitrogen and phosphorus removal from municipal wastewater effluent using microalgal biofilms, Water Res. 45 (2011) 5925–5933.

[8] J.P. Gustafsson, A. Renman, G. Renman, K. Poll, Phosphate removal by mineral-based sorbents used in filters for small-scale wastewater treatment, Water Res. 42 (2008) 189–197.

[9] L.D. Hylander, A. Kietlińska, G. Renman, G. Simán, Phosphorus retention in filter materials for wastewater treatment and its subsequent suitability for plant production, Bioresour. Technol. 97 (2006) 914–921.

[10] C. Nilsson, G. Renman, L.J. Johansson Westholm, A. Renman, A. Drizo, Effect of organic load on phosphorus and bacteria removal from wastewater using alkaline filter materials, Water Res. 47 (2013) 6289–6297.

[11] A. Renman, L.D. Hylander, G. Renman, Transformation and removal of nitrogen in reactive bed filter materials designed for on-site wastewater treatment, Ecol. Eng. 34 (2008) 207–214.

[12] A. Renman, G. Renman, Long-term phosphate removal by the calcium-silicate material Polonite in wastewater filtration systems, Chemosphere 79 (2010) 659–664.

[13] M. Kõiv, M. Liira, Ülo Mander, R. Mõtlep, C. Vohla, K. Kirsimäe, Phosphorus removal using Ca-rich hydrated oil shale ash as filter material—The effect of different phosphorus loadings and wastewater compositions, Water Res. 44 (2010) 5232–5239.

[14] E.H. Kim, D.W. Lee, H.K. Hwang, S. Yim, Recovery of phosphates from wastewater using converter slag: Kinetics analysis of a completely mixed phosphorus crystallization process, Chemosphere 63 (2006) 192–201.

[15] E.H. Kim, S.B. Yim, H.C. Jung, E.J. Lee, Hydroxyapatite crystallization from a highly concentrated phosphate solution using powdered converter slag as a seed material, J. Hazard. Mater. 136 (2006) 690–697.

[16] U. Berg, D. Donnert, A. Ehbrecht, W. Bumiller, I. Kusche, P.G. Weidler, R. Nüesch, "Active filtration" for the elimination and recovery of phosphorus from waste water, Colloid. Surf., A 265 (2005) 141–148.

[17] W.G. Fu, P.P. Li, Characteristics of phosphorus adsorption of aerated concrete in wastewater treatment, Adv. Mater. Res. 183–185 (2011) 466–470.

[18] S. Malavipathirana, S. Wimalasiri, N. Priyantha, S. Wickramasooriya, A. Welagedara, G. Renman, Value addition to waste material supported by removal of available phosphate from simulated brackish water—A low cost approach, J. Geosci. Environ. Prot. 01 (2013) 7–12.

[19] E. Oğuz, A. Gürses, N. Canpolat, Removal of phosphate from wastewaters, Cem. Concr. Res. 33 (2003) 1109–1112.

[20] G. Renman, A. Renman, Sustainable use of crushed autoclaved aerated concrete (CAAC) as a filter medium in wastewater purification, in: WASCON 2012 Conference proceedings, 2012.